

1 **CRISPR/Cas9-based silencing of the *ATXN1* gene in Spinocerebellar ataxia type 1 (SCA1)**  
2 **fibroblasts**

3  
4 Francesca Salvatori<sup>1</sup>, Mariangela Pappadà<sup>1</sup>, Mariaconcetta Sicurella<sup>1</sup>, Mattia Buratto<sup>1</sup>, Valentina  
5 Simioni<sup>2</sup>, Valeria Tugnoli<sup>2</sup> & Peggy Marconi<sup>1\*</sup>

6  
7 <sup>1</sup>Department of Chemical and Pharmaceutical Sciences, University of Ferrara, via Fossato di Mortara  
8 64/B, 44121 Ferrara, Italy.

9 <sup>2</sup>Department of Neuroscience and Rehabilitation, Division of Neurology, University Hospital of  
10 Ferrara, via A. Moro 8, 44100, Cona, Ferrara, Italy.

11 **Corresponding author mailing address: [peggy.marconi@unife.it](mailto:peggy.marconi@unife.it)**

12  
13 **Abstract**

14 Spinocerebellar Ataxia type 1 (SCA1) is an autosomal dominant neurodegenerative disorder caused  
15 by a gain-of-function protein with toxic activities, containing an expanded polyQ tract in the coding  
16 region. Actually, there are no treatments available to delay the onset, stop or slow down the  
17 progression of this pathology. Many approaches developed over the years involve the use of siRNAs  
18 and antisense oligonucleotides (ASOs). Here we develop and validate a CRISPR/Cas9 therapeutic  
19 strategy in fibroblasts isolated from SCA1 patients. We started from the screening of 10 different  
20 sgRNAs able to recognize regions upstream and downstream the CAG repeats, in exon 8 of *ATXN1*  
21 gene. The two most promising sgRNAs, G3 and G8, whose efficiency was evaluated with an *in vitro*  
22 system, significantly downregulated the ATXN 1 protein expression. This downregulation was due  
23 to the introduction of indels mutations into the *ATXN1* gene. Notably, with an RNA-seq analysis, we  
24 demonstrated minimal off-target effects of our sgRNAs. These preliminary results support  
25 CRISPR/Cas9 as a promising approach for treated polyQ-expanded diseases.

26 **Abbreviations**

27 SCA1: Spinocerebellar Ataxia type 1

28 ATXN1: ataxin 1

29 PolyQ: polyglutamine

30 ASO: antisense oligonucleotide

31 sgRNA: single guide RNA

32 CRISPR: clustered regularly interspaced short palindromic repeat

33 Cas: CRISPR associated proteins

34 RNP: ribonucleoprotein

## 35 **Introduction**

36 SCA1 is an autosomal dominant neurodegenerative disorder caused by a CAG-repeat expansion in  
37 *ATXN1* gene. The severity of the disease and its onset are directly proportional to the number of  
38 triplets. The mutated *ATXN1* contains an expanded polyQ tract and shows new toxic functions which  
39 lead to neurodegeneration [Orr, 2000; Zoghbi and Orr, 2009]. PolyQ SCAs, which have a frequency  
40 of 2-3 cases per 100.000 people, are progressive, typically striking in midlife and causing increasing  
41 neuronal dysfunction and eventual neuronal loss 10-20 years after onset of symptoms [Zoghbi and  
42 Orr, 2000]. Patients can lose the ability to breathe in a coordinated fashion, which can be fatal [Orr,  
43 2012].

44 Currently, no treatments are available to prevent or cure, delay the onset, stop or slow down the  
45 progression of these diseases. Several research groups are trying to develop strategies to reduce the  
46 levels of mutated proteins, and therefore their neurotoxic effects, using for example antiaggregant  
47 agents [Zoghbi and Orr, 2000], molecules capable of activating the ubiquitin-proteasome pathway  
48 [Nagashima et al., 2011] and compound with autophagic effects, as lithium [Watase et al., 2007],  
49 tensirolimus [Menzies et al., 2010], thehalose [Chen et al., 2015] and Beclin-1 [Nascimento-Ferreira  
50 et al., 2011].

51 Potential genetic therapies for SCA1 involve several different nucleic acid-based molecules able to  
52 target the RNA or DNA of the polyQ-associated genes. Since methods exploiting the mechanisms  
53 involved in the processing of endogenous miRNAs, as siRNAs and shRNAs, have shown potential  
54 toxicity [Grimm et al., 2010], antisense oligonucleotide-mediated (ASO-mediated) RNA suppression  
55 approaches have been recently used to reduce gene expression and improve disease symptoms in  
56 preclinical rodent models of several neurological diseases [Friedrich et al., 2018; McLoughlin et al.,  
57 2018], including SCA1 [Friedrich et al., 2018]. The disadvantage of these methods lies in the need  
58 for continuous administration throughout the patient's life, to keep toxic protein levels low.

59 To address this fundamental limitation, the field of gene editing has emerged to make precise, targeted  
60 modifications to genome sequences. The most popular and used tool for gene editing currently is the  
61 clustered regularly interspaced short palindromic repeat (CRISPR)/Cas9 system [Jinek et al., 2012].  
62 The CRISPR/Cas9, a component of the bacterial RNA-mediated adaptive immune system, consists  
63 of transcribed guide RNAs that direct the Cas9 RNA-guided DNA endonuclease to target sequences  
64 [Jinek et al., 2012; Barrangou et al., 2007]. The CRISPR/Cas9 system from *Streptococcus pyogenes*  
65 has already been successfully used in treating genetic disorders [Jinek et al., 2012; Jinek et al., 2013].

66

67

68

## 69 **Results**

### 70 **Design and *in vitro* screening of sgRNAs**

71 We designed ten different sgRNAs able to recognize sequences upstream and downstream the *ATXN1*  
72 polyQ tract (Fig. 1A), using the CRISPR design software developed by Zhang lab [Brezelton et al.,  
73 2015], and tested the efficiency to recognise and mediate the cutting by Cas9 of these sgRNAs in *in*  
74 *vitro* reactions. The efficiencies shown in figure 1b were determined as a percentage of the fragments  
75 obtained from the Cas9 cut related to the total amount of the target sequence. At least, four sgRNAs  
76 show a high capacity to mediate the cut of the target sequence (G3, G8, G10, G11), two of which  
77 recognize sequences upstream and two downstream of the polyQ tract. Since a multiple cut of the  
78 *ATXN1* gene can determine loss of genetic material and therefore a more efficient silencing of the  
79 gene itself [Maeder and Gersbach, 2016], we set up four pairs of sgRNAs, whose recognition and  
80 cutting efficiency was always very high (Fig. 1C). From preliminary tests on U266 cellular line, we  
81 chose the G3-G8 sgRNA pair which confirmed the ability to effectively knock-out *ATXN1* gene  
82 expression (data not shown).

83

### 84 **Isolation and characterization of SCA1 fibroblasts**

85 Fibroblasts were isolated from a 4 mm skin fragment, obtained from five patients, after the signature  
86 of the informed consent, with different polyQ expansion in mutated *ATXN1* gene: SCA1N1 (50  
87 repeats), SCA1N5 (45), SCA1N6 (42), SCA1N8 (60), SCA1N17 (67).

88 To confirm the presence of an *ATXN1* allele with pathological increase in CAG triplets we amplified  
89 by PCR the exon 8 of the *ATXN1* gene and verified, by electrophoresis on agarose gel, the presence  
90 of two PCR fragments, one due to the healthy allele and one to the mutated one (Fig. 2a). At the same  
91 time, to verify the production of the wild type and expanded polyQ ataxin 1, a western blotting  
92 experiment was set up, where using anti-ATXN1 antiserum 12NQ it was possible to highlight the  
93 presence of both ATXN1 proteins (Fig. 2a).

94

### 95 **Validation of CRISPR/Cas9-based therapeutic strategy in SCA1 fibroblasts**

96 Fibroblasts were then transfected with G3 and G8 sgRNA simultaneously and with a negative control  
97 sgRNA, as nucleofection control, previously associated with a Cas9 to obtain ribonucleoproteins  
98 (RNPs). Western blotting analysis with anti-ATXN1 antiserum 12NQ, using total protein amount and  
99 anti-HSP90 for normalization, showed significant reduction of the ATXN1 expression (from 27,2%  
100 to 75,2% of expression compared to not treated cells) (Fig. 3a,b).

101 To verify which genetic alterations were introduced by our CRISPR/Cas9 system, we decided to  
102 amplify the region of exon 8 containing the polyQ and the sequences recognized by G3 and G8 of the

103 treated cells of three patients and to subclone PCR products. Following sequencing and alignments  
104 with the correct exon sequence, we were able to determine in what percentage indels and point  
105 mutations were introduced or the polyQ was completely excised (Fig. 3c-e), obtaining  $13\% \pm 4\%$  for  
106 indels,  $14\% \pm 5\%$  for point mutations and  $2\% \pm 2\%$  for polyQ deletions.

107

### 108 **Evaluation of off-target effects**

109 To verify if the G3 and G8 Cas9/sgRNA complexes determined a significant alteration in the  
110 expression of off-target genes, we carried out transcriptome profiling of the treated versus not treated  
111 fibroblasts of three patients by RNA-seq, performed by Lexogen. From a minimum of 5.44 to a  
112 maximum of 6.9 million uniquely mapped reads were carried out, for a total of approximately 1600  
113 genes. Figure 4a displays inter-replicate correlations plots. The overall correlation of expression  
114 between samples which were defined as replicates is very good.

115 Differential expression analysis (Fig. 4b) was normalised using the DESeq methods [Anders and  
116 Huber, 2010], which ignore highly variable and/or highly expressed features. From this analysis it  
117 emerged that only two genes are significantly altered by treatment with Cas9/sgRNA complexes:  
118 *TXNIP* up regulated and *HAS2* down regulated about twice.

119

### 120 **Discussion**

121 SCA1 is one of the two spinocerebellar ataxias with the highest incidence in Italy, especially in the  
122 North, with a frequency of around 21% [Brusco et al., 2004]. It is also present with a high relative  
123 prevalence in Russia, South Africa, Serbia and India [Di Donato et al., 2012]. There is no cure for  
124 SCA1, and current therapies only provide symptomatic relief. Although several research teams are  
125 trying to develop therapeutic strategies that can silence the *ATXN1* gene and block the production of  
126 the toxic protein, none of these approaches have entered clinical trials, neither in Europe  
127 [<https://www.clinicaltrialsregister.eu/>] nor in the United States [<https://clinicaltrials.gov/>].

128 Recent studies have shown that polyQ-expanded ATXN1 exerts cerebellar toxicity mainly through  
129 its interaction with CIC [Rousseaux et al., 2018], therefore, genetic approaches aimed at blocking the  
130 production of this protein seem to be the most promising strategies for the treatment of SCA1. Since  
131 it has already been shown that specific CRISPR/Cas9-mediated gene editing could be used to  
132 permanently eliminate polyglutamine expansion-mediated neuronal toxicity [Ouyang et al., 2018;  
133 Yang et al., 2017], we successfully developed a CRISPR/Cas9-based approach to efficiently reduce  
134 the production of both healthy and mutated ATXN1 protein.

135 This therapeutic genome-editing strategy is not able to discriminate between the mutated and wild  
136 type allele of the *ATXN1* gene, but in any case, it has already been shown that a partial suppression  
137 of both forms of the ATXN1 protein is well tolerated [Keiser et al., 2016].

138 Our approach involves the use of two different sgRNAs targeting exon 8 of the *ATXN1* gene [Maeder  
139 and Gersbach, 2016] and, analysing the gene modifications introduced by our CRISPR/Cas9 system  
140 to the *ATXN1* gene, we found that the two sgRNAs seem to have different efficiency to recognise the  
141 target sequence and mediate the Cas9 cut. G3 and G8 sgRNAs mediate the excision of the polyQ tract  
142 only very few times (only 5% in SCA1N8), probably due to the steric hindrance caused by the  
143 nearness of the target sequences and the high molecular weight of the Cas9. G3 sgRNA showed a  
144 higher efficacy (with a ratio of about 3 to 1) and the largest number of indel and/or point mutations  
145 were localized upstream the polyQ tract compared to the cut mediated by G8 sgRNA downstream of  
146 the polyQ. Moreover, to verify if the lower efficiency of G8 was due to a guide design error, we  
147 analysed the theoretical efficiency of this sgRNA using all the software currently available for RNA  
148 design guides [Brazelton et al., 2015]. This analysis demonstrated the good theoretical efficiency of  
149 the G8 confirming our hypothesis that, in association with G3, there is a competition between the two  
150 guides and the dimensions of Cas9 which reduce the effectiveness of the G8. Therefore, we are  
151 designing a new RNA guide capable of recognizing a sequence much further downstream than that  
152 recognized by G8, in order to minimize the steric hindrance of the two sgRNA/Cas9 complexes.

153 Although the CRISPR/Cas9 system has a minimal incidence of off-target effects [Kadam et al., 2018],  
154 variable levels of the latter have been observed [Fu et al., 2013; Hsu et al., 2013; Lin et al., 2014].  
155 The Cas9 endonucleases produced in recent times are engineered to increase their efficiency towards  
156 the target sequence, minimizing the off-target effects. Furthermore, accurate design of sgRNAs and  
157 the direct delivery of the ribonucleoprotein complex, whose short half-life considerably reduces the  
158 exposure time of the cell genome to the action of the CRISPR/Cas9 system, can significantly reduce  
159 any off-target effects [Brazelton et al., 2015]. From the RNA-seq analysis, performed on three cell  
160 samples treated with G3/Cas9 and G8/Cas9 RNPs, we identified two genes whose expression was  
161 significantly, albeit in a limited way, altered by treatment: *HAS2*, downregulated, and *TXNIP*,  
162 upregulated. Since none of these are reported as possible off-site targeting of our system, we  
163 hypothesized that their variation is due to the suppression of the mutated ATXN1 protein and its toxic  
164 functions. Further studies will be done to investigate this aspect and to confirm that our silencing  
165 system can restore wild type conditions at the level of protein expression.

166 In conclusion, in this study we demonstrate to successfully reduce protein expression from SCA1  
167 patient-specific cells using the CRISPR/Cas9 system, obtaining suppression efficiencies that agree  
168 with those obtained by Friedrich et al. when treated *Atxn154Q/2Q* mice with the antisense

169 oligonucleotide ATXN1 ASO353 [Friedrich et al., 2018], but with the advantage of permanent  
170 suppression, without the need of continuous administration. However, these results will be confirmed  
171 in SCA1 fibroblasts of other patients that have been already recruited.

172 The CRISPR/Cas9 system is proving to be an effective and powerful technique for modifying genes.  
173 The use of the gene editing system in dominant inherited ataxias like SCA1, where the polyQ  
174 expansion in exon 8 of *ATXN1* leads to a gain of toxic protein function, may be the only solution for  
175 these neurodegenerative diseases.

176

## 177 **Materials and Methods**

### 178 **sgRNA design and screening**

179 sgRNAs were designed by CRISPR Design software, developed by Zhang at the MIT Laboratory in  
180 2015 [Brezelton et al., 2015]. To test the efficacy of designed sgRNA, Guide-it In Vitro Transcription  
181 and Screening Kit (Takara Bio USA, Mountain View, California) was used, according to the  
182 manufacturer's protocol.

183

### 184 **Sample-size estimation**

185 The calculation of the sample size was made, assuming a 30% variation in efficacy in the treatment  
186 compared to the negative control, a 1st type error  $\alpha$  equal to 0.05 and a power  $\beta$  of 0.80. The sample  
187 size calculation was equal to 5 cell samples.

188

### 189 **Skin biopsy**

190 Patients underwent skin biopsy at the distal leg, 10 cm above the lateral malleolus, using a disposable  
191 4-mm punch under sterile condition after local anaesthesia with lidocaine. The procedure does not  
192 need suture. Specimens were transferred into 15 ml tubes containing DMEM high glucose medium  
193 supplemented with 20% fetal bovine serum (FBS), antibiotic and antimycotic solution, and then taken  
194 to the laboratory to be processed. All subjects signed the informed consent and the studies were  
195 approved by the AVEC ethics committee.

196

### 197 **Fibroblasts isolation**

198 The skin fragments were transferred to a 10 cm diameter cell plate and further fragmented with a  
199 disposable scalpel. The skin fragments were then moved into two T25 flasks with 1 ml of medium.  
200 Fresh medium was added after 48 hours and at regular intervals until it reached 3 - 4 ml in total, after  
201 which it was replaced twice a week. After 20-25 days, fibroblasts were detached with Trypsin-EDTA

202 1X (EuroClone, Pero, Italy) and moved to a new flask. New medium was added to the plate with skin  
203 fragments and fibroblasts were periodically transferred to new flasks for at least a month. Once  
204 amplified, SCA1 patient-derived fibroblasts were frozen as passage 1.

205

## 206 **Cell culture and transfection**

207 SCA1 skin fibroblasts were maintained in DMEM high glucose medium supplemented with 20%  
208 FBS, antibiotic and antimycotic solution. 80 pmoles of Cas9 were complexed with 240 pmoles of  
209 sgRNA, incubating at room temperature (RT) for 20 minutes. RNP complexes were transfected in  
210 500,000 cells with Amaxa Nucleofector II (Amaxa Biosystems, Lonza, Basel Switzerland) using the  
211 P-022 program according to manufacturer's protocol and adding 1 ul of 100  $\mu$ M Alt-R<sup>®</sup> Cas9  
212 Electroporation Enhancer (IDT, Coralville, Iowa), followed by plating in 6 well plates. The cells were  
213 then amplified for at least 7-10 days until a sufficient number of cells was obtained, from which both  
214 genomic DNA and total proteins were extracted.

215

## 216 **Western blotting analyses**

217 Protein extracts were prepared by homogenization of cellular precipitates in extraction buffer (50 mM  
218 Tris-HCl pH 8.0, 1% V/V Triton X-100, 0.5% V/V Nonidet P-40, 10 mM mercaptoethanol, 4% V/V  
219 glycerol and Complete Mini Protease inhibitor cocktail tablets (Roche, Basel Switzerland), 1 tablet  
220 in 10 mL), followed by five freeze/thaw cycles and then centrifuged at 4°C for 3 min at 14,000 rpm.  
221 Supernatants were quantified by Pierce<sup>™</sup> BCA Protein Assay Kit (Thermo Fisher Scientific,  
222 Waltham, Massachusetts) and used for Western blotting analysis, using for the ATXN1 detection the  
223 antiserum 12NQ, kindly donated by Dr. Orr [Perez Ortiz et al., 2018], and the antibody against HSP90  
224 (Biosciences Inc., Allentown, Pennsylvania), as housekeeping. 30  $\mu$ g of protein extracts were  
225 denatured for 5 minutes at 98°C in 1X SDS sample buffer (62.5 mM Tris-HCl pH 6.8, 2% SDS, 50  
226 mM Dithiothreitol (DTT), 0.01 % bromophenol blue, 10% glicerol), resolved by SDS-PAGE and  
227 transferred to nitrocellulose membranes (BioRad Laboratories Inc., Hercules, California). After  
228 blocking with 3% skim milk/TBS, the membranes were incubated with primary antibodies in 1%  
229 skim milk/TBS overnight at 4°C. After washing in 0.05% Tween 20/TBS, membranes were incubated  
230 with the corresponding secondary antibody conjugated with HRP in 1% skim milk/TBS for 1 hr at  
231 RT and washed again. Chemiluminescence signals were detected using the Clarity Western ECL  
232 Substrate (BioRad Laboratories Inc.) according to the manufacturer's protocol. The signal intensity  
233 was determined using the ChemiDoc MP Imaging System (BioRad Laboratories Inc.) and ATXN1  
234 expression in treated cells compared to not treated ones was calculated using for normalization both  
235 total proteins amount and HSP-90.

236

### 237 **Phenol/chloroform extraction of genomic DNA**

238 Cell pellets were resuspended with a lysis solution (10 mM Tris HCl pH 8.0, 400 mM NaCl, 2 mM  
239 EDTA pH 8.0, 0.45% p/V SDS and 0.45 mg/mL proteinase K) and incubated at 56°C for 2 hours.  
240 One volume of phenol:chloroform:isoamyl alcohol (25:24:1) was added and mixed by inversion for  
241 5 minutes. Samples were centrifuged at RT for 5 minutes at 12,000 rpm and then the aqueous phase  
242 was transferred to a clean tube. After a second extraction to optimize DNA purification, an equal  
243 volume of chloroform:isoamyl alcohol was added to the aqueous phase and samples were centrifuged  
244 under the same conditions described above. 2.5 volumes of 96% ethanol were added to each tube,  
245 which were placed at -20°C overnight to precipitate DNA. Samples were centrifuged at 4°C for 5  
246 minutes at 12,000 rpm, washed with 1 ml of 70% ethanol and then centrifuged again under the same  
247 conditions. The dry pellets were finally resuspended in water and the DNA quantified using the  
248 Biospectrometer (Eppendorf, Hamburg, Germany).

249

### 250 **PCR**

251 PCR products were amplified in 100 µl reactions with 0.2 units of EconoTaq DNA polymerase  
252 (Lucigen, Middleton, Wisconsin), 1 µM of each primer, and 0.25 mM of each dNTP. Thermal cycling  
253 was done using an annealing temperature of 56°C. PCR products were purified using NucleoSpin®  
254 Gel and PCR Clean-up (Macherey-Nagel, Hoerd, France), according to manufacturer's protocol.

255

### 256 **PCR subcloning**

257 Purified PCR fragments were cloned into a pGEM-T Easy Vector (Promega, Madison, Wisconsin),  
258 according to the manufacturer's protocol. The ligation reactions were then transformed into E. coli  
259 5-alpha Chemically Competent cells (Lucigen), performing a thermal shock for 45 seconds at 42°C  
260 followed by 2 minutes on ice. After 1 hours at 37°C in slow agitation, bacteria were plated in 100  
261 ng/µl ampicillin LB-Agar plates, with 0.01% X-gal/200 µM IPTG.

262 White colonies were amplified and plasmids purified using PureYield™ Plasmid Miniprep System  
263 (Promega), according to the manufacturer's protocol. The obtained plasmids were analysed through  
264 electrophoresis in 0.8% agarose gel, quantified using the Biospectrometer (Eppendorf) and send to  
265 BMR Genomics for sequencing, set up using the M13 forward sequencing primer.

266

### 267 **Total RNA extraction**

268 The total cellular RNA was extracted by TRIZOL® Reagent (Gibco - Thermo Fisher Scientific),  
269 according to manufacturer's protocol. All reagents and materials used were RNase-free. The extracted



270 RNA was analysed by electrophoresis on 0.8% agarose gel and sent to Lexogen (Greenland, New  
271 Hampshire) for RNA-seq analyses.

272

### 273 **Statistical analysis**

274 Statistical analyses were performed using GraphPad Prism 7.00 software. The statistical tests applied  
275 were: unpaired t test with two-tailed P value and alpha level  $P < 0.05$ ; F test to compare variances with  
276 alpha level  $P < 0.05$ .

277

### 278 **Acknowledgements**

279 We thank Harry T. Orr for providing us with anti-ATXN1 antiserum 12NQ for our western blotting  
280 experiments.

281

### 282 **Funding**

283 This work was supported by A.C.A.RE.F. Foundation onlus and AISA onlus.

284

### 285 **Competing interests**

286 All the authors declare no competing financial interests.

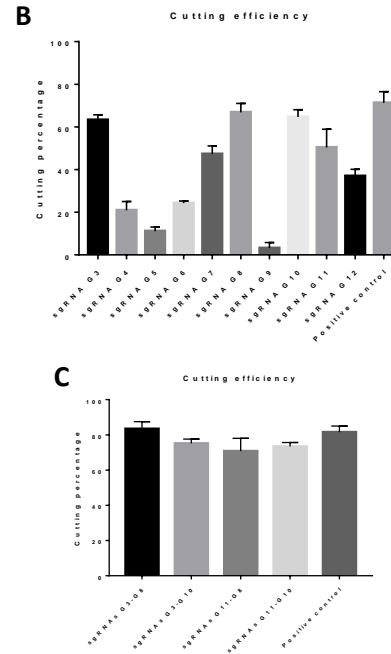
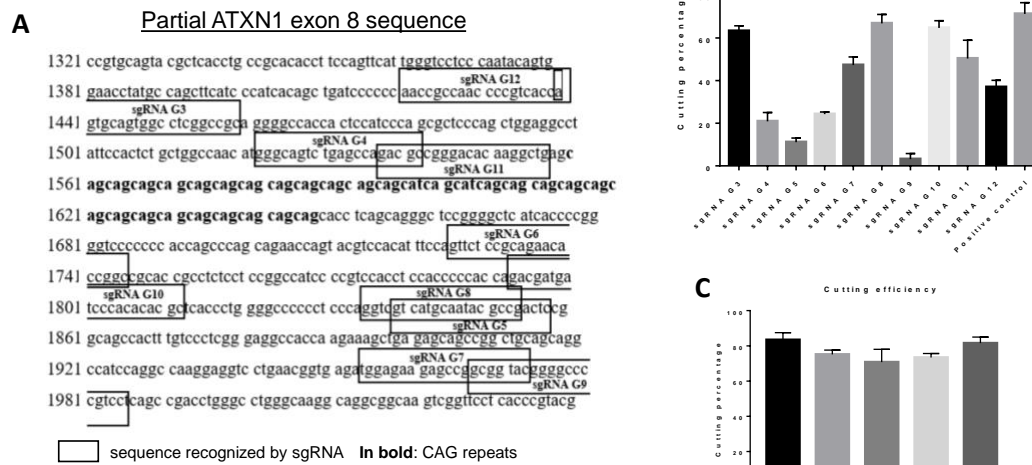
287

### 288 **References**

- 289 Anders S, Huber W. Differential expression analysis for sequence count data. *Genome Biol* 2010; 11:  
290 R106.
- 291 Barrangou R, Fremaux C, Deveau H, Richards M, Boyaval P, Moineau S, et al. CRISPR provides  
292 acquired resistance against viruses in prokaryotes. *Science* 2007; 315: 1709-1712.
- 293 Brazelton VA Jr., Zarecor S, Wright DA, Wang Y, Liu J, Chen K, et al. A quick guide to CRISPR  
294 sgRNA design tools. *GM Crops Food* 2015; 6: 266-276.
- 295 Brusco A, Gellera C, Cagnoli C, Saluto A, Castucci A, Michielotto C, et al. Molecular Genetics of  
296 Hereditary Spinocerebellar Ataxia: Mutation Analysis of Spinocerebellar Ataxia Genes and  
297 CAG/CTG Repeat Expansion Detection in 225 Italian Families. *Arch Neurol* 2004; 61(5):  
298 727-33.
- 299 Chen ZZ, Wang CM, Lee GC, Hsu HC, Wu TL, Lin CW, et al. Trehalose attenuates the gait ataxia  
300 and gliosis of spinocerebellar ataxia type 17 mice. *Neurochem Res* 2015; 40: 800-810.

- 301 Di Donato S, Mariotti C, Taroni F. Spinocerebellar ataxia type 1. In: Aminoff MJ, Boller F, Swaab  
302 DF, editors. Handbook of Clinical Neurology. Amsterdam: ELSEVIER BV 2012; 103: 399-  
303 421.
- 304 Friedrich J, Kordasiewicz HB, O'Callaghan B, Handler HP, Wagener C, Duvick L, et al. Antisense  
305 oligonucleotide-mediated ataxin-1 reduction prolongs survival in SCA1 mice and reveals  
306 disease-associated transcriptome profiles. JCI Insight 2018; 3(21): e123193.
- 307 Fu Y, Foden JA, Khayter C, Maeder ML, Reyon D, Joung JK, et al. High-frequency off-target  
308 mutagenesis induced by CRISPR-Cas nucleases in human cells. Nat Biotechnol 2013; 31:  
309 822-826.
- 310 Grimm D, Wang L, Lee JS, Schürmann N, Gu S, Börner L, et al. Argonaute proteins are key  
311 determinants of RNAi efficacy, toxicity, and persistence in the adult mouse liver. J Clin Invest  
312 2010; 120: 3106-3119.
- 313 Hsu PD, Scott DA, Weinstein JA, Ran FA, Konermann S, Agarwala V, et al. DNA targeting  
314 specificity of RNA-guided Cas9 nucleases. Nat Biotechnol 2013; 31: 827-832.
- 315 Jinek M, Chylinski K, Fonfara I, Hauer M, Doudna JA, Charpentier E. A programmable dual-RNA-  
316 guided DNA endonuclease in adaptive bacterial immunity. Science 2012; 337: 816-821.
- 317 Jinek M, East A, Cheng A, Lin S, Ma E, Doudna J. RNA-programmed genome editing in human  
318 cells. Elife 2013; 2: e00471.
- 319 Kadam, US, Shelake, RM, Chavhan, RL, Suprasanna, P. Concerns regarding 'off-target' activity of  
320 genome editing endonucleases. [Review]. Plant Physiol Biochem 2018; 131: 22-30.
- 321 Keiser MS, Monteys AM, Corbau R, Gonzalez-Alegre P, Davidson BL. RNAi Prevents and Reverses  
322 Phenotypes Induced by Mutant Human ataxin-1. Ann Neurol 2016; 80(5): 754-765.
- 323 Lin Y, Cradick TJ, Brown MT, Deshmukh H, Ranjan P, Sarode N, et al. CRISPR/Cas9 systems have  
324 off-target activity with insertions or deletions between target DNA and guide RNA sequences.  
325 Nucleic Acids Res 2014; 42: 7473-7485.
- 326 Maeder ML, Gersbach CA. Genome-editing Technologies for Gene and Cell Therapy. [Review]. Mol  
327 Ther 2016; 24: 430-446.
- 328 McLoughlin HS, Moore LR, Chopra R, Komlo R, McKenzie M, Blumenstein KG, et al.  
329 Oligonucleotide therapy mitigates disease in spinocerebellar ataxia type 3 mice. Ann Neurol  
330 2018; 84: 64-77.
- 331 Menzies FM, Huebener J, Renna M, Bonin M, Riess O, Rubinsztein DC. Autophagy induction  
332 reduces mutant ataxin-3 levels and toxicity in a mouse model of spinocerebellar ataxia type  
333 3. Brain 2010; 133: 93-104.

- 334 Nagashima Y, Kowa H, Tsuji S, Iwata A. FAT10 protein binds to polyglutamine proteins and  
335 modulates their solubility. *J Biol Chem* 2011; 286: 29594-29600.
- 336 Nascimento-Ferreira I, Santos-Ferreira T, Sousa-Ferreira L, Auregan G, Onofre I, Alves S, et al.  
337 Overexpression of the autophagic beclin-1 protein clears mutant ataxin-3 and alleviates  
338 Machado-Joseph disease. *Brain* 2011; 134: 1400-1415.
- 339 Orr HT. The ins and outs of a polyglutamine neurodegenerative disease: spinocerebellar ataxia type  
340 1 (SCA1). [Review]. *Neurobiol Dis* 2000; 7: 129-134.
- 341 Orr HT. Cell biology of spinocerebellar ataxia. [Review]. *J Cell Biol* 2012; 197: 167-177.
- 342 Ouyang S, Xie Y, Xiong Z, Yang Y, Xian Y, Ou Z, et al. CRISPR/Cas9-targeted deletion of  
343 polyglutamine in spinocerebellar ataxia type 3-derived induced pluripotent stem cells. *Stem*  
344 *Cells and Development* 2018; 27(11): 756-770.
- 345 Perez Ortiz JM, Mollema N, Toker N, Adamski CJ, O'Callaghan B, Duvick L, et al. Reduction of  
346 protein kinase A-mediated phosphorylation of ATXN1-S776 in Purkinje cells delays onset of  
347 Ataxia in a SCA1 mouse model. *Neurobiol Dis* 2018; 116: 93-105.
- 348 Rousseaux MW, Tschumperlin T, Lu HC, Lackey EP, Bondar VV, Wan YW, et al. ATXN1-CIC  
349 Complex Is the Primary Driver of Cerebellar Pathology in Spinocerebellar Ataxia Type 1  
350 Through a Gain-of-Function Mechanism. *Neuron* 2018; 97(6): 1235-1243.
- 351 Watase K, Gatchel JR, Sun Y, Emamian E, Atkinson R, Richman R et al. Lithium therapy improves  
352 neurological function and hippocampal dendritic arborization in a spinocerebellar ataxia type  
353 1 mouse model. *PLoS Med* 2007; 4: e182.
- 354 Yang S, Chang R, Yang H, Zhao T, Hong Y, Kong HE, et al. CRISPR/Cas9-mediated gene editing  
355 ameliorates neurotoxicity in mouse model of Huntington's disease. *J Clin Invest* 2017; 127:  
356 2719-2724.
- 357 Zoghbi HY, Orr HT Glutamine repeats and neurodegeneration. [Review]. *Annu Rev Neurosci* 2000;  
358 23: 217-247.
- 359 Zoghbi HY, Orr HT. Pathogenic mechanisms of a polyglutamine-mediated neurodegenerative  
360 disease, spinocerebellar ataxia type 1. [Review]. *J Biol Chem* 2009; 284: 7425-7429.
- 361
- 362
- 363

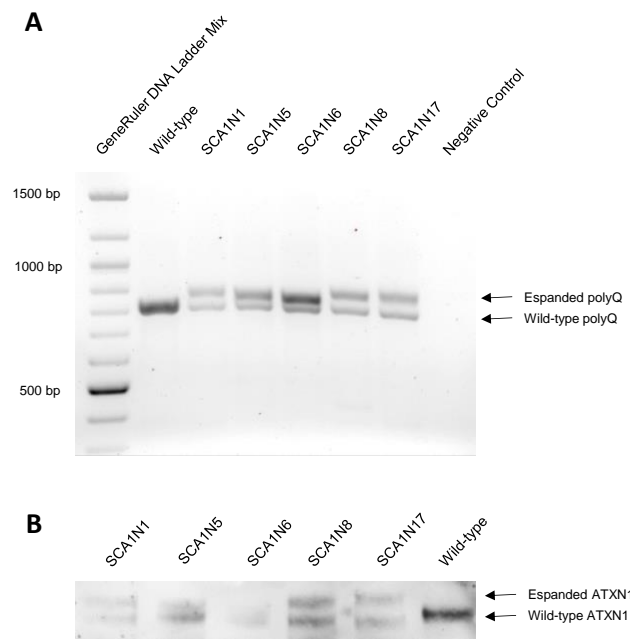


364

365 **Figure 1. Design and *in vitro* screening of sgRNAs for ATXN1 gene.** **A**, sgRNAs were designed  
366 using the CRISPR design software by Zhang lab. Ten sgRNAs capable of cutting upstream and  
367 downstream of the polyQ tract were identified. **B**, Using Guide-it sgRNA *In Vitro* Transcription and  
368 Screening System (Clontech), *in vitro* screening tests were performed to evaluate the sgRNAs cutting  
369 efficiency, which were  $63,3 \pm 1,4$  (G3),  $20,9 \pm 2,4$  (G4),  $11,1 \pm 1,1$  (G5),  $24,3 \pm 0,6$  (G6),  $47,3 \pm 2,2$   
370 (G7),  $66,8 \pm 2,4$  (G8),  $3,2 \pm 1,5$  (G9),  $64,7 \pm 2,0$  (G10),  $50,4 \pm 4,9$  (G11),  $37,0 \pm 1,8$  (G12). **C**, The  
371 most efficient sgRNAs were then tested in pairs. The cutting efficiencies were  $83,4 \pm 2,4$  (G3-G8),  
372  $75,2 \pm 1,4$  (G3-G10),  $70,8 \pm 4,2$  (G11-G8),  $73,4 \pm 1,3$  (G11-G10). Values are mean  $\pm$  s.e.m. from at  
373 least three independent experiments.

374

375



376

377 **Figure 2. Characterization of SCA1 fibroblasts.** A, Amplification by PCR of the *ATXN1* exon 8  
378 containing the polyQ tract, using the genomic DNA extracted from the five SCA1 patients' fibroblasts  
379 as template. A, ATXN1 expression in SCA1 fibroblasts, using 12NQ antiserum as anti-ATXN1  
380 antibody.

381

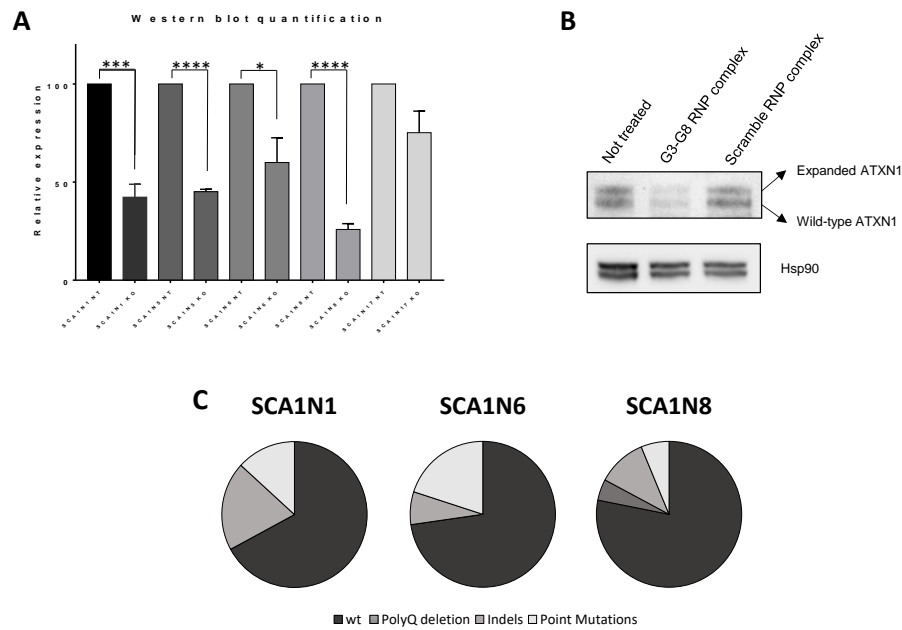
382

383

384

385

386

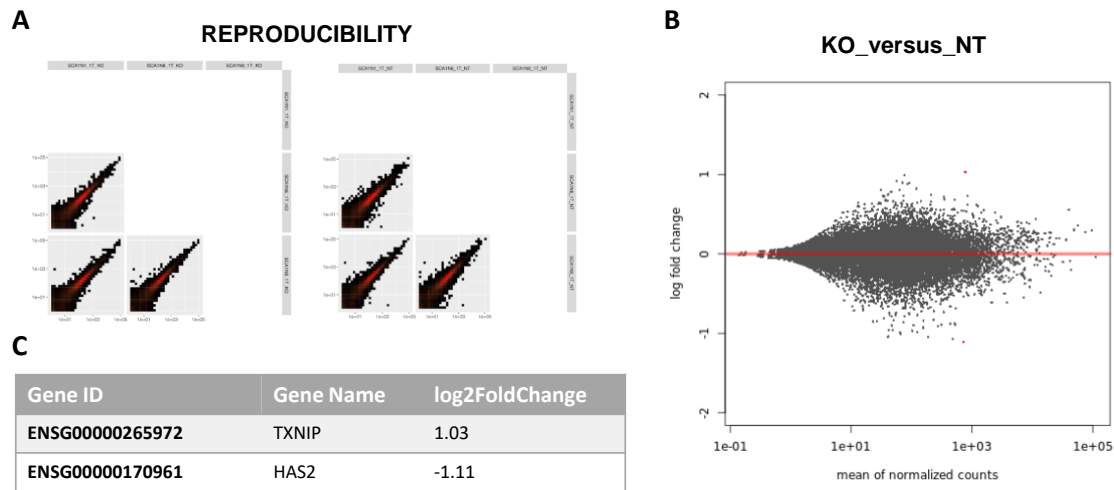


387

388 **Figure 3. Effects of CRISPR/Cas9 system in SCA1 fibroblasts. A-B,** Atxn1 expression in SCA1  
 389 fibroblast. Fibroblasts from five SCA1 patients were treated using sgRNAs G3 and G8 complexed  
 390 with Cas9 endonucleases and the Atxn1 expression was determined by Western Blotting. **A,** Atxn1  
 391 abundances were expressed relative to Hsp90 and total proteins, determined by densitometry. After  
 392 the treatment, the Atxn1 expression was  $42,3 \pm 3,8$  (SCA1N1),  $46 \pm 2,6$  (SCA1N5),  $60 \pm 5$  (SCA1N6),  
 393  $23,7 \pm 2,6$  (SCA1N8) and  $75,2 \pm 4,8$  (SCA1N17). **B,** Expression in patient SCA1N1 for Atxn1 and  
 394 HSP90. **C-E,** Mutations introduced by CRISPR/Cas9 system in ATXN1 genes of three patients and  
 395 their relative abundance, determined by sequencing 76 (**C**), 55 (**D**) and 64 (**E**) colonies. Values are  
 396 mean  $\pm$  s.e.m. from at least three independent experiments. \*P=0,05, \*\*\*P<0,001, \*\*\*\*P<0,0001,  
 397 unpaired t test followed by f test to compare variances.

398

399



400

401 **Figure 4. Transcriptome profile by RNA-seq.** **A**, Inter-replicate correlation plots, which verify the  
402 overall correlation of expression between replicates. **B**, Digital gene expression data can be visualized  
403 as MA plot, just as with microarray data where each dot represents a gene. This plot shows RNA-seq  
404 gene expression for sgRNA/Cas9 treated versus not treated SCA1 fibroblasts. The red dots  
405 correspond to the only two differentially expressed genes, following treatment, showing in table **C**.

406

407

408

409

410